23rd ABCM International Congress of Mechanical Engineering
December 6-11, 2015, Rio de Janeiro, RJ, Brazil

FATIGUE ANALYSIS OF DYNAMIC SYSTEMS SUBJECTED TO CYCLIC LOADING IN THE FREQUENCY DOMAIN

U. L. Rosa[1]
A.M.G. de Lima[2]
Federal University of Uberlândia, School of Mechanical Engineering, Campus Santa Mônica, 38400-902, Uberlândia, MG, Brazil
[1]*ulisses.ufu@hotmail.com*
[2]*amglima@mecanica.ufu.br*

Abstract. *The design of engineering systems depends on a number of factors, highlighting the environment where it will work and how it will be loaded. Considering structures subjected to random loadings one of the major problems is the material failure by fatigue that occurs with no previous notice and generally on a sudden and catastrophic way. On this case, the analysis and characterization of the phenomenon require the application of statistical methods. The interest of this contribution is to describe fatigue in thin plates. A model is developed applying classical finite elements method and fatigue estimation by Sines' criterion. This process requires Fourier's domain analysis of the system, using stress power spectral densities (PSD) of the structure submitted to a white Gaussian noise random loading. After the theoretical developments, the numerical results obtained by using a thin plate subjected to random multiaxial Gaussian loads are presented.*

Keywords: *fatigue, random vibrations, stress PSD, Sines criterion, finite elements method.*

1. INTRODUCTION

The greatest part of tests concerning material strains and stresses requires gradual quasi-static charge application. Besides that, loadings are applied only once and the specimen is destructed (Budynas and Nisbett, 2011). These tests can estimate material's static properties such as elastic modulus, elastic limits, stiffness and toughness. However, they actual don't approximate real conditions that most structures are subjected.

Failure occurs when one machine, structure or material cannot perform its designed function anymore, but it is often and mostly associated with complete breaking (Affonso, 2002). They are generally caused by negligence during the concept and construction or by the application of new designs and materials (Anderson, 2005). Although negligence may be avoided by several methods, the second failure cause is more difficult to prevent and requires special attention in mechanical engineering.

Dimensioning a structure for static loadings is not a complex process since the modulus and limits are available for most materials. On the other hand, if there is any kind of random or variable loading actuating, the generated stresses vary with time or fluctuate between levels and so the fatigue phenomenon starts to be a problem because its failure maximum stresses are below the material's ultimate strength and even bellow its yield strength (Budynas and Nisbett, 2011). Fatigue is caused by generation and propagation of cracks and is accelerated by effects of environment and frequency of cycling. This phenomenon's biggest problem is that it occurs generally on a very dangerous, sudden and catastrophic way, without previous notice (Dowling, 2007).

Lambert (2007) pointed out that cracks usually appear on critical points where the stress levels are higher and there are few ways to predict them. One way is working on time domain, analyzing stress historic and comparing with the S-N diagram. This is entirely possible but impracticable due to high time spent on data acquisition and post treatment. Another approach and a viable one is to obtain data from frequency domain, specifically by statistical analysis of the structure's stress spectral power density (stress PSD).

Sines (1959) proposed a stress criterion for multiaxial fatigue that consists on the calculation of a factor that is function of the square root of the stress deviation tensor second invariant, the hydrostatic stresses and material parameters related to fatigue tests. The method developed by Li and de Freitas (2002) considers the non-proportionality of the loading on the estimation of this second invariant. Its calculations involves spectral moments obtained directly from the stress PSD. There are other fatigue criteria developed through the years but Sines' criterion still generates accurate results with a simpler formulation (Weber, 1999).

A thin plate finite elements model submitted to white Gaussian noise random loading was developed and the results obtained generated excellent approximations for the FRF and stress PSDs of the structure. After all, the PSDs are used to apply Sines' criterion for multiaxial loads on Fourier's domain, generating a contour map of the plate with the probability of failing for each element.

2. FINITE ELEMENTS METHOD FORMULATION

The studied structure is a thin plate modeled by Kirchhoff's theory (Zienkiewicz and Taylor, 2005) and discretized by plane rectangular five degrees-of-freedom-per-node elements ($u_0, v_0, w_0, \theta_x, \theta_y$). In order to model mechanical displacement fields, the classical Finite Elements Method (FEM) was used. They are given by Eq. (1).

$$\boldsymbol{u}(x,y,z,t) = u_0 + z\theta_x \tag{1.a}$$

$$\boldsymbol{v}(x,y,z,t) = v_0 + z\theta_y \tag{1.b}$$

$$\boldsymbol{w}(x,y,z,t) = w_0 \tag{1.c}$$

Elements on the right side of the equations are obtained for each node inside each element. They are approximated by shape functions denoted $\boldsymbol{N}(x,y)$ as shown on Eq. (2).

$$\boldsymbol{U}(x,y,z,t) = \boldsymbol{A}(z)\boldsymbol{N}(x,y)\boldsymbol{u_e}(t) \tag{2}$$

where $\boldsymbol{A}(z)$ is a matrix containing the parameter z and $\boldsymbol{u_e}(t)$ is the vector containing nodal displacement data.

The ordinary differential equation represented on Eq. (3) governs the undamped structure's movement and its solution estimates the displacement field.

$$\boldsymbol{M\ddot{U}} + \boldsymbol{KU} = \boldsymbol{F} \tag{3}$$

where $\boldsymbol{U}$ is the nodal displacement vector and $\boldsymbol{\ddot{U}}$ its second time derivative, $\boldsymbol{F}$ is the applied load vector, $\boldsymbol{M}$ and $\boldsymbol{K}$ are the mass and stiffness global matrices respectively.

These two matrices follow developments based on energy variational approaches (kinetic energy for the mass and potential energy for stiffness) applied on FEM models. Elemental matrices shown on Eq. (4) and (5) are lately assembled by the system's connectivity, composing the global matrices (Faria, 2006).

$$\boldsymbol{M_e} = \int_{V_e} \rho \boldsymbol{N}(x,y)^T \boldsymbol{N}(x,y) dV_e \tag{4}$$

$$\boldsymbol{K_e} = \frac{1}{2}\int_{Ve} \dot{\boldsymbol{N}}(x,y)^T \boldsymbol{H}\ \dot{\boldsymbol{N}}(x,y)\ dV_e \tag{5}$$

where $\boldsymbol{H}$ is the mechanical properties matrix, depending on the structure's material.

After all displacement fields have been determined by the equations above, it is possible to obtain strain fields. They are related to $\boldsymbol{U}(x,y,z,t)$ by the use of derivatives shown on Eq. (6).

$$\begin{Bmatrix} \varepsilon_x \\ \varepsilon_y \\ \gamma_{xy} \end{Bmatrix} = \begin{bmatrix} \partial/\partial x & 0 & 0 \\ 0 & \partial/\partial y & 0 \\ \partial/\partial y & \partial/\partial x & 0 \end{bmatrix} \begin{Bmatrix} u \\ v \\ w \end{Bmatrix} = \boldsymbol{D}\,\boldsymbol{U}(x,y,z,t) \tag{6}$$

being $\boldsymbol{D}$ the differential matrix above and $\boldsymbol{\varepsilon}(x,y,z,t)$ the elemental strain vector.

We may define the matrix $\boldsymbol{B}(x,y,z) = \boldsymbol{D}\,\boldsymbol{A}(z)\boldsymbol{N}(x,y)$ and rewrite Eq. (6) as seen on Eq. (7).

$$\boldsymbol{\varepsilon}(x,y,z,t) = \boldsymbol{B}(x,y,z)\boldsymbol{u_e}(t) \tag{7}$$

Equation (8) represents Hooke's law application to the strain field obtained on Eq. (7), obtaining the stress fields for each element of the structure.

$$\boldsymbol{\sigma}(x,y,z,t) = \boldsymbol{H}\,\boldsymbol{\varepsilon}(x,y,z,t) \tag{8}$$

3. STRESS RESPONSES

Obtaining time responses by the equations shown on section 2 demands high computational efforts, so it is highly recommended working on Fourier's frequency domain (Lambert, 2007). To a closer reality approach, it is convenient to add a structural damping to Eq. (3). For the studied thin plate, it is introduced in the system as a proportional damping obtained directly from a coefficient multiplying the stiffness matrix $(\boldsymbol{C}=\beta\boldsymbol{K})$. Equation (9) represents the full model.

$$\boldsymbol{M}\ddot{\boldsymbol{U}}+\boldsymbol{C}\dot{\boldsymbol{U}}+\boldsymbol{K}\boldsymbol{U}=\boldsymbol{F} \tag{9}$$

Applying Fourier's transform to Eq. (9) the system's frequency response is obtained. It is represented on Eq. (10).

$$\boldsymbol{U}(\omega)=\left[-\omega^2\boldsymbol{M}+j\omega\boldsymbol{C}+\boldsymbol{K}\right]^{-1}\boldsymbol{F}(\omega) \tag{10}$$

where $\boldsymbol{U}(\omega)$ and $\boldsymbol{F}(\omega)$ are the Fourier's transform of the displacement and the applied loading, respectively.

Now we define the structure's frequency response function (FRF) on Eq. (11).

$$\boldsymbol{G}(\omega)=\left[-\omega^2\boldsymbol{M}+j\omega\boldsymbol{C}+\boldsymbol{K}\right]^{-1} \tag{11}$$

Spectral density functions can be defined via correlation functions. This is a method assuming that autocorrelation and cross-correlation functions of the system exist (Bendat and Piersol, 2010). The calculated spectral density is defined on the interval $(-\infty,+\infty)$ and have symmetry properties. As negative frequencies are not interesting on this kind of analysis, it is convenient to introduce the one-sided spectral function, defined on $[0,+\infty)$. Its values are always double of the two-sided spectral function evaluated on positive frequencies.

The system's power spectral density matrix of displacement $\boldsymbol{\phi}_u(\omega)$ is shown on Eq. (12).

$$\boldsymbol{\phi}_u(\omega)=\int_{-\infty}^{+\infty}\boldsymbol{R}_u(\tau)e^{-j\omega t}d\tau \tag{12}$$

where $\boldsymbol{R}_u$ is the autocorrelation function of the displacement field, submitted to a load *f(t)* with autocorrelation function $\boldsymbol{R}_f$. On time domain its value is given by Eq. (13).

$$\boldsymbol{R}_u(\tau)=\int_{-\infty}^{+\infty}\int_{-\infty}^{+\infty}\boldsymbol{g}(\lambda)\boldsymbol{R}_f(\tau+\lambda-\zeta)\boldsymbol{g}^T(\zeta)d\lambda d\zeta \tag{13}$$

where $\boldsymbol{g}(t)=\dfrac{1}{2\pi}\displaystyle\int_{-\infty}^{+\infty}\boldsymbol{G}(\omega)e^{j\omega t}d\omega$ is the system's impulse response.

Rearranging Eqs. (12) and (13), using Fourier transform definitions and spectral density properties (Lambert, 2007) it is possible to formulate Eq. (14), relating the displacement PSD, load PSD $\boldsymbol{\phi}_f(\omega)$ and system's FRF.

$$\boldsymbol{\phi}_U(\omega)=\boldsymbol{G}(\omega)\left(\int_{-\infty}^{+\infty}\boldsymbol{R}_f(\tau)e^{j\omega t}d\tau\right)\boldsymbol{G}^H(\omega)=\boldsymbol{G}(\omega)\boldsymbol{\phi}_f(\omega)\boldsymbol{G}^H(\omega) \tag{14}$$

All finite elements equations established for time domain on section 2 are valid on frequency domain as well. Applying Fourier transform on Eqs. (7) and (8), expressions for frequency analysis of strains and stresses are obtained. After introducing them on Eq. (14), it is possible to formulate stress PSD $\boldsymbol{\phi}_S(\omega)$ shown on Eq. (15).

$$\boldsymbol{\phi}_S(\omega)=\boldsymbol{H}\,\boldsymbol{B}\,\boldsymbol{G}(\omega)\,\boldsymbol{\phi}_f(\omega)\,\boldsymbol{G}^H(\omega)\,\boldsymbol{B}^T\boldsymbol{H}^T \tag{15}$$

4. SINES' FATIGUE CRITERION

Uniaxial fatigue criteria with zero mean can be obtained directly from the S-N diagram (also known as Wöhler diagram, (Budynas and Nisbett, 2011)). If the structure is subjected to multiaxial loadings, there are different methods of fatigue life estimation. The most accepted and efficient uses tensor invariants, usually the first invariant of the stress tensor (I_1) or the second invariant of the deviation tensor (J_2). Weber (1999) pointed out on his studies several criteria and noticed that the best results were obtained by Fogue's and Sines' criteria.

Fogue's criterion presented slightly better results than Sines' but requires three material properties on his formulation, making it very restrict. On the other hand, Sines' criterion uses octahedral plan as the maximum shear plane and its formulation is simple, reducing computational time and effort. It also needs only two material properties related to fatigue (alternate torsional ($t_{\_1}$) and alternate traction ($f_{\_1}$) fatigue resistance).

On his work, Sines (1959) established a coefficient called D_{Sines} that express the probability of fatigue failure. It is statistically calculated due to random loadings. So instead of calculating it directly, what is needed is its expected value, given by Eq. (16) (Lambert, 2007).

$$E[D_{Sines}] = \frac{E[\sqrt{J_{2,a}}] + \alpha E\left[p(t)\right]}{A} \tag{16}$$

where $\sqrt{J_{2,a}}$ is the estimation of the square root of the second deviation tensor invariant, $p(t)$ is the hydrostatic stress, $A = t_{-1}$, $\alpha = \dfrac{3t_{-1}(R_m + f_{-1})}{f_{-1}R_m} - \sqrt{6}$ and R_m is the ultimate material's strength.

Li and de Freitas (2002) proposed a method of evaluating $\sqrt{J_{2,a}}$ using the minimum circumscribed ellipse method. This method can be expanded for five-dimension prismatic hull circumscribing the loading path of $\sqrt{J_{2,a}}$. Equation (17) is used to estimate its value (Lambert et al., 2010).

$$E\left[\sqrt{J_{2,a}}\right] = \sqrt{E\left[R_1\right]^2 + E\left[R_2\right]^2 + E\left[R_3\right]^2 + E\left[R_4\right]^2 + E\left[R_5\right]^2} \tag{17}$$

Each semi-axe R_i of the prismatic hull is obtained by Eq. (18).

$$E\left[R_i\right] \approx \lambda_{0,i}\left(\sqrt{2\ln N_p\left(\tilde{D}_i(t)\right)} + \frac{\gamma}{\sqrt{2\ln N_p\left(\tilde{D}_i(t)\right)}}\right), i = 1,\ldots,5 \tag{18}$$

where $\lambda_{0,i}$ is the zero-order spectral moment, $\gamma = 0.5772$ is the Euler-Mascheroni constant and $N_p\left(\tilde{D}_i(t)\right)$ is the number of maxima on the gaussian process $\tilde{D}_i(t)$, estimated by Eq. (19).

$$N_p\left(\tilde{D}_i(t)\right) = \frac{T}{2\pi}\sqrt{\frac{\lambda_{1,i}{}^2}{\lambda_{2,i}{}^2}}, i = 1,\ldots,5 \tag{19}$$

with $\lambda_{1,i}$ and $\lambda_{2,i}$ the first and second order spectral moments obtained from stress PSDs.

5. RESULTS AND DISCUSSION

5.1 Model Presentation

In this section simulations were performed with a thin rectangular aluminum plate. It is sized $0.654m \times 0.527m$ and the discretization used on the modeling is a 12×12 plane rectangular finite elements mesh with four nodes and five degrees of freedom per node, comprising a total number of 845 DOF. A proportional damping with $\beta = 2.5x10^{-4}$ was considered on the model. Double clamping along y axis is assumed as boundary conditions. The plate's mechanical properties are given on Tab. 1 and a simplified schema regarding its axis and meshing is depicted in Fig. 1.

Table 1. Mechanical properties of the aluminum plate

Thickness (mm)	Young's Module (GPa)	Poisson ratio	Mass density (kg/m³)	Ultimate strength limit (MPa)	Alternate torsional limit[1] (MPa)	Alternate traction limit[1] (MPa)
1.5	70	0.33	2700	343	92	132

[1]obtained for 2.0×10^6 cycles

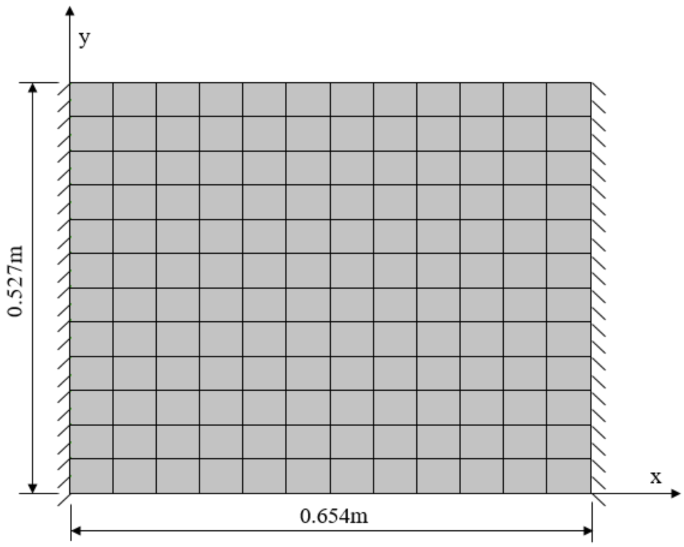

Figure 1. Thin plate simplified schema and meshing

5.2 Frequency Response Function (FRF)

The objective of the first analysis is to obtain displacement FRFs of the system. It is developed applying the concept defined on Eq. (11). Its main purpose is to generate data that will be used lately to calculate stress response on the frequency domain. To validate this results, the FRF's peaks must match with the natural frequencies ω_n obtained by the solution of Eq. (20), which is an eigenvalue problem associated with Eq. (3).

$$[K - \omega^2 M] = 0 \tag{20}$$

The first ten natural frequencies are presented on Tab. 2.

Table 2. First ten natural frequencies of the thin plate

Mode	Frequency [Hz]
1	19.2081
2	24.4506
3	47.5554
4	53.0939
5	60.6489
6	86.4604
7	96.8855
8	104.4579
9	112.8357
10	134.3635

Solving this model with all its DOF requires heavy computational efforts due to matrix inversions, so it is convenient to reduce the model. Gerges (2013) pointed out several reduction methods and the best adapted to a linear thin plate is applying Ritz basis. This basis reduces the system and all the matrices on Eq. (9). It is composed of nodal displacements of vibration (eigenvectors of Eq. (20)) and is enriched with static residues. The number of modes considered depends on the accuracy needed. The more modes inserted the closer to reality the system is but takes more computation time. It is usual to analyze 1.5 times the desired frequency range and to consider all the vibration modes inside it. The interest frequency range is 0-100 Hz, so it is recommended to work on a 0-150 Hz range and all the modes below 150 Hz must be used on the basis composition. So it was composed with the first ten vibration modes plus the static residue for a unitary load applied on the central node. Therefore, the system was reduced from 845 to 11 effective degrees of freedom.

As a matter of comparison, both full and reduced system's FRFs due to a unitary impulse applied and measured on the central node and are shown on Fig. 2.

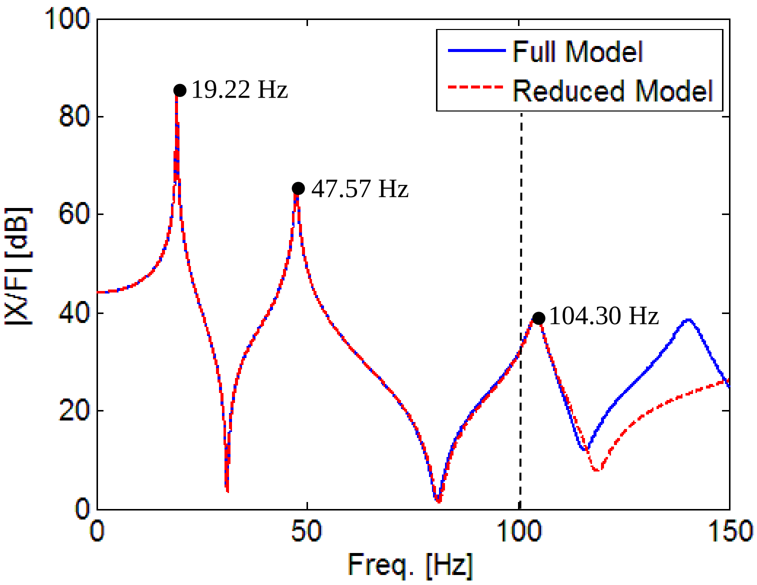

Figure 2. Comparison between full and reduced finite elements method

As desired, an excellent approximation is noted in Fig. 2 on the 0-100 Hz frequency range. The first three peaks plotted correspond to the first, third and eighth vibration modes, respectively. These values are not exactly the same as those on Tab. (2) due to the number of points used on the FRF discretization. If a larger number of points is used, more accurate results are obtained.

As expected, after the 100 Hz dashed line the reduced model starts to differ. If more accuracy is needed it is recommended working in a larger frequency range, including more vibration modes in the reduction basis. This method provided a 90% computational time gain, making possible the generation of the FRFs and PSDs in a more effective way.

5.3 Effect of Thickness on Stress Responses

The second analysis consists on obtaining stress responses on the frequency domain for each one of the plate's elements. Stress PSDs of the thin plate model are obtained by Eq. (15). The system was loaded with a white Gaussian noise with $\phi_f(\omega) = 85x10^3$ Pa²/Hz. Figure 3 shows how σ_{xx} and σ_{yy} normal tension curve's shape and magnitude change for three different simulations with different thickness (1.5mm, 2.0mm and 2.5mm).

The other plate's dimensions remains the same, hence higher thickness reflects directly on higher mass and stiffness. This explains why the natural frequencies values increase as well as the stress levels get lower. For fatigue life analysis, it is expected thicker structures with lower tension levels to have less chance of breaking.

5.4 Sines' Fatigue Criterion

Stress response data were obtained for each one of the 144 elements. This allows the first step in order to apply Sines' fatigue. They are used on Eqs. (17), (18) and (19) to estimate the expected value for $\sqrt{J_{2,a}}$. After its calculation, Eq. (16) may be applied. For each element one value of $E[D_{Sines}]$ is generated. All the values were contour-plotted on Fig. 4, making easier to locate the probable failure points.

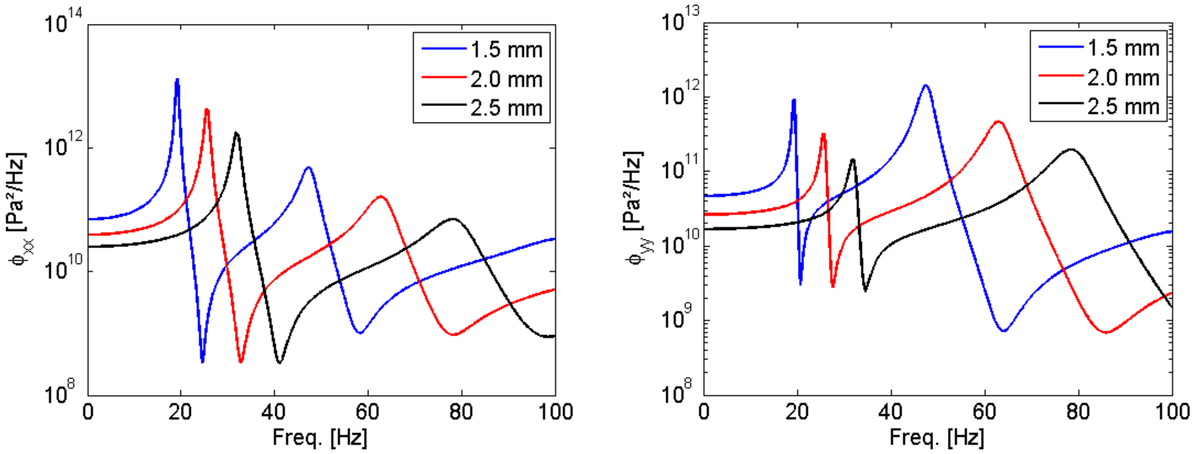

Figure 3. Normal stress levels behavior with thickness increase for an element in the center of the plate

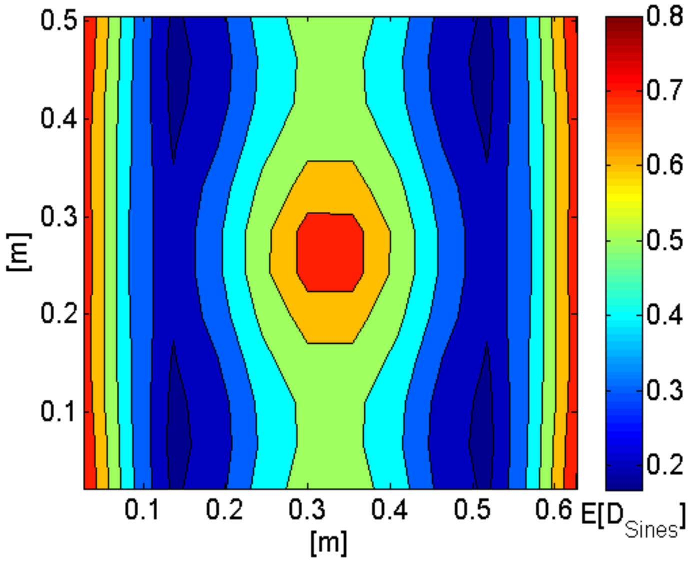

Figure 4. Expectation of Sines coefficient distribution among the plate's elements

Analyzing Fig. (4), it is noted that higher values for the Sines' coefficient are grouped around the load application point and the plate's clamped borders. As expected, this happens because these elements are where higher tension values due to cycling excitation are found. The closer these values are to the unit, the greater is the probability of breaking after two million cycles.

6. CONCLUDING REMARKS

A model concerning finite elements frequency analysis of displacements, strain and stresses in order to apply statistical methods regarding fatigue criteria application has been suggested. Numerical simulations showed that it is efficient and provided accurate and effective results for a thin aluminum plate with a white Gaussian noise load. This study is relevant for the aerospace industry, for example for sonic fatigue analysis, fatigue cracking prevention and control.

7. ACKNOWLEDGEMENTS

The authors are grateful for Federal University of Uberlândia (UFU), Laboratório de Mecânica das Estruturas José Eduardo Tannus Reis (LMest) and Instituto Nacional de Ciência e Tecnologia de Estruturas Inteligentes em Engenharia (INCT-EIE) for the opportunity and support given to the realization of this research work and to CAPES (Coordenação de Aperfeiçoamento de Pessoal de Nível Superior), CNPq (Conselho Nacional de Desenvolvimento Científico e Tecnológico) and FAPEMIG (Fundação de Amparo à Pesquisa do Estado de Minas Gerais) for the financial support.

8. REFERENCES

Affonso, L. O. A., 2002. *Equipamentos Mecânicos: Análise de Falhas e Solução de Problemas*. Qualitymark, Rio de Janeiro.

Anderson, T. L., 2005. *Fracture Mechanics: Fundamentals and Applications*. Taylor & Francis, 3rd edition.

Bendat, J. S. and Piersol, A.G., 2010. *Random Data: Analysis and Measurements Procedures*. John Wiley & Sons, New Jersey, 4th edition.

Budynas, R. G. and Nisbett, J. K., 2011. *Shigley's Mechanical Engineering Design*. McGraw-Hill, New York, 9th edition.

Dowling, N. E., 2007. *Mechanical Behavior of Materials: Engineering Methods for Deformation, Fracture and Fatigue*. Pearson Prentice Hall, 3rd edition.

Gerges, Y., 2013. *Méthodes de reduction de modèles en vibroacoustique non-linéaire*. Ph.D. thesis, Université de Franche-Comté, Besançon.

Lambert, S., 2007. *Contribution à l'analyse d l'endommagement par fatigue et au dimensionnement de structures soumises à des vibrations aléatoires*. Ph.D. thesis, INSA de Rouen, Rouen.

Lambert, S., Pagnacco E. and Khalij, L., 2010. "A probabilistic model for the fatigue reliability of structures under random loadings with phase shift effects". *International Journal of Fatigue*, Vol. 32, p. 463-474.

Li, B. and de Freitas, M., 2002. "A procedure for fast evaluation of high-cycle fatigue under multiaxial random loading". *Journal of Mechanical Design*, Vol. 124, p. 558-563.

Sines, G., 1959. "Behavior of Metals Under Complex Static and Alternating Stresses", In *Metal Fatigue*, McGraw-Hill, New York.

Weber, B., 1999. *Fatigue multiaxiale des structures industrielles sous chargement quelconque*. Ph.D. thesis, INSA de Lion, Lion.

Zienkiewicz, O.C. and Taylor, R. L., 2005. *The Finite Element Method for Solid and Structural Mechanics*. Elsevier Butterworth-Heinemann, Oxford, 6th edition.

9. RESPONSIBILITY NOTICE

The authors are the only responsible for the printed material included in this paper.